Planetary Nebulae: An Eye to the Future
Proceedings IAU Symposium No. 238, 2011
A. Manchado, L. Stanghellini & D. Schönberner, eds.

doi:10.1017/S1743921312010721

AGB mass loss

Lee A. Willson and Qian Wang

Department of Physics and Astronomy, Iowa State University,
Ames, , Iowa, USA 50010
email: lwillson@iastate.edu

Abstract. Mass loss on the AGB removes most of the envelope and leaves a compact remnant to become a white dwarf and perhaps first the central star of a planetary nebula. The envelope mass provides an upper limit on the material available to form the PN, and the terminal mass loss rate plus the small remnant mass left on the core determines how much of that would still be available to form the PN after the star has evolved far enough to the blue. Given a mass loss formula based on observations or models, we can find the deathline where $-dM_{\rm star}/dt = (M/L)\,dL/dt$ and can find the contours of constant mass loss rate on a plot of M vs. L. From such plots we can derive the mass available for a PN and the lowest mass single star that can produce a PN of a given mass. However, some details important for PN formation remain uncertain, including the maximum mass loss rate achieved and the envelope mass left when AGB mass loss ceases.

Keywords. Stars: mass loss, stars: AGB and post-AGB, Miras, stars: winds, outflows

1. Introduction

The study of mass loss on the AGB for single stars can yield several results of interest for the study of planetary nebulae: (a) the timing of mass loss (all at the end, or spread out over RGB/AGB evolution) can affect the composition of the nebula; (b) the luminosity and core mass of a star that has reached devastating mass loss rates determine the masses of planetary nebulae nuclei (PNNi) from single stars (if any) and, generally, the initial-final mass relation; (c) the maximum rate of mass loss achieved gives some limits on which stars could possibly form PNe without companions; and (d) the final rates of mass loss have a bearing on the transition time for the central star from the AGB to the region of PNNi. This review will concentrate on what we know, from observations and models, about (b) and (c).

The first dynamical models with mass loss were computed in the late 1970s, by Steve Hill (Hill & Willson 1979; Willson & Hill 1979, collectively = HW). Wood (1979) also examined the case where shocks and radiation pressure on dust were both present in the atmosphere. Three cases were considered: Isothermal shocks, adiabatic shocks, and (HW) a transition from isothermal at high gas density to adiabatic at low gas density. It was evident from these models that periodic isothermal shocks produced aperiodic shock patterns and minimal mass loss; while adiabatic shocks from the photosphere ejected most of the atmosphere each cycle. The hybrid-cooling models produced mass loss rates within an order of magnitude or so of the right amount. Isothermal models with dust added also produced significant mass loss (Wood 1979).

Insights from the above led to another round of modeling for the pulsating AGB stars. Bowen (1988) developed a code that included density-dependent (non-LTE) cooling, dust formation, and the pulsation dynamics. Other groups concentrated on getting a better handle on the dust physics, particularly for carbon stars where the laboratory data on nucleation and growth were more complete (Fleischer *et al.* 1992; Gail & Sedlmayr 1999; Höfner & Dorfi 1997; Höfner *et al.* 1995). Today, very sophisticated codes treating dust

nucleation and chemistry in some detail and/or including detailed, non-grey, radiative transfer are in use for comparison with a wealth of observational data, while current computer capabilities allow simpler codes to be used for very extensive parameter studies of the processes involved. (For detailed models, see Höfner *et al.* 2003; Mattsson *et al.* 2010; Mattsson & Höfner 2011.)

Until recently, most of the very detailed modeling was for carbon-star atmospheres, and an interesting problem arose when these were adapted for use on oxygen-rich stars: It appeared to be impossible to produce the mass loss rates that are observed (Woitke 2006). The Bowen code had no such difficulty. While there is still some debate on this point, the resolution of this problem appears to involve several important bits: (a) For the carbon stars, the acceleration produced by scattering of photons is very small compared to that produced by absorption, and in some versions of the carbon star codes the scattering terms had been turned off. (b) In order for the silicate grains to have sufficient opacity, they need to be either contaminated by iron or they need to be larger than those produced in the detailed carbon star models. Contamination by iron does not work because to get enough iron for the opacity leads to overheating and sublimation of the grains, but size does work (Höfner 2009). (c) The Bowen models have used mainly the Rosseland mean opacity to obtain the unperturbed density structure and the photospheric density in the dynamical models scales with this parameter; this is a small opacity and gives a high photospheric density and high mass loss rates. The more detailed radiative transfer codes typically have lower photospheric densities and thus lower mass loss rates for similar stellar parameters. We are exploring the effects of using smaller opacity in our new large grid of Bowen-code models.

Another complication of terminal AGB mass loss is the modulation of L and R by shell flashes – typically a cycle of 10^5 years with up to 1000 years of elevated L, 10^4 years of depressed L during helium shell burning, then a gradual rise to a plateau value for quiescent hydrogen burning. The main effect of this is that stars spend 10% of their time at significantly lower mass loss rates, i.e. out of the death zone, during the ascent. A smaller effect is the short period of elevated mass loss rate during the high-L episode; however, even with large $d\log\dot{M}/d\log L$ the amount lost during the short, high-L state is not more than 10%, roughly offsetting the low L time. (We define $\dot{M} = -dM_{\rm star}/dt$.) The expected range of mass loss rate over the shell flash cycle is just $(d\log\dot{M}/d\log L)$ $\Delta\log L$ since the star travels along the same $R(L, M)$ at fixed composition. Observations of detached shells (Olofsson *et al.* 1990) confirm this general picture.

An advantage of the Bowen code is that apart from the numerical value of each parameter there is nothing in the code that specifies that the star must have a certain composition. Thus, by changing the $R(L, M, Z)$, the atmospheric mean opacity, and the dust condensation parameters $T_{\rm cond}$ and $\Delta T_{\rm cond}$ we can equally well model a carbon star as an M star. The only reason we have not yet done so is that we expect $R(L, M, Z)$ to have a large effect and we do not yet know $d\log R/d\log({\rm C/O})$. However, studies that have been undertaken already by Marigo (2002) will provide this information and we will then be able to follow the effect on mass loss rates of the changing composition of the star. It is already evident that the radii of the carbon stars will be significantly larger at a given L, and from that fact we can confidently predict that (1) if a star has entered the death zone before becoming a carbon star then it will rapidly lose all its mass as C/O rises; and (2) the death zone for carbon stars will fall at lower L than for M stars of the same mass, meaning that the initial-final mass relation could be non-monotonic.

Mass loss formulae used for "synthetic AGB evolution" include those based on observational data (Reimers 1975; Vassiliadis & Wood 1993) and those based on model grids (Wachter 2002; Willson 2007; Willson & Wang in prep). One can crudely characterize

https://doi.org/10.1017/S1743921312010721 Published online by Cambridge University Press

the mass loss history of stars leaving the AGB in terms of (i) mass loss below the first RGB tip; (ii) mass loss at the He core flash; (iii) mass loss along the AGB before the last 200,000 years; and (iv) mass loss in the death-zone at the tip of the AGB. In each stage, we want to know both ΔM, the net mass lost, and some dependence of the mass loss rate on stellar parameters, such as a (local) power law fit $\dot{M} = -dM/dt = aL^bM^{-c}Z^d$ along an evolutionary track $R(L, M, Z, l/H)$.

2. AGB tip mass loss

It is evident from observations that the stars at the tip of the AGB are generally losing mass at rates that will remove their envelopes in times comparable to the e-folding time of the luminosity, $-(1/M)dM/dt \sim (1/L)dL/dt \sim 5 \times 10^{-7}$ yr^{-1}. We are currently running large grids of models with parametrized physics for key processes, and find it convenient to summarize the results of many models in terms of $L_{\rm death}$, $d\log\dot{M}/d\log L$ along a constant-mass evolutionary track at $L_{\rm death}$, $d\log\dot{M}/d\log M$ at $L_{\rm death}$, and $d\log\dot{M}/d\log Z$ at $L_{\rm death}$. We call $d\log\dot{M}/d\log L$ along a constant-mass evolutionary track the "slope" of the mass loss law, and $d\log\dot{M}/d\log M$ is the exponent for the mass-dependence. We define the deathline $L_{\rm death}(M)$ as where $(1/M)dM/dt \sim (1/L)dL/dt \sim 5 \times 10^{-7}$ yr^{-1} and the death-zone as the range of $L(M)$ over which the mass loss rate $\dot{M}$ increases from $0.1(M/L)dL/dt$ to $10(M/L)dL/dt$.

Typical parameters of our models, and death-lines and power law fits to some other mass loss formulae from the literature, are presented in Table 1. Although it is clear at this time that the Reimers formula cannot account for AGB tip mass loss, we include it because it has been so widely used in evolutionary and population studies.

In Figure 1 we show the effects of varying the slope $d\log\dot{M}/d\log L$ (for constant M evolving in L), and the mass exponent $d\log\dot{M}/d\log L$ (at constant L), on the terminal evolution of the AGB, for four combinations inspired by the values of Table 1. The mass available to form a PN is no more than the amount lost during the last 10^4 years. If we assume that there is an upper limit to the mass loss rate of 3×10^{-5} M$_\odot$ yr^{-1}, then we can estimate the maximum PN masses vs. M for each case. As argued by Moe (this proceedings) there is a lower limit on the progenitor mass that can produce a PN with a mass of a few tenths of a solar mass, and this lower limit is sensitive to the mass loss law; the larger the slope and mass-exponent, the smaller the lower limit on possible progenitor masses.

3. Effects of modeling parameters on the results

Our grid of models is designed to let us investigate the effect on mass loss rates and outflow speeds of a variety of hard-to-model processes: Convection and nonlinear pulsation in the interior; radiative transfer, non-LTE and dust formation in the atmosphere. Each of these is described in our code with one or more equations containing a parameter that can be compared with results from more detailed calculations of each process. Detailed calculations tell us a range of reasonable values to consider for each parameter, and we can then see how much leverage ($d\log\dot{M}/d\log X$ times the range of X) each parameter provides on the results.

Convection enters via mixing length theory and its parameter is l/H; Iben's AGB star relation has $d\log R/d\log(l/H) = -0.52$. Nonlinear pulsation determines the amplitude of motion of the lowest zone in the model, sometimes referred to as the piston. We have used two specifications for the piston amplitude, one valid for the majority of lower mass-loss-rate models and one more appropriate for the highest mass loss rates and/or lowest

https://doi.org/10.1017/S1743921312010721 Published online by Cambridge University Press

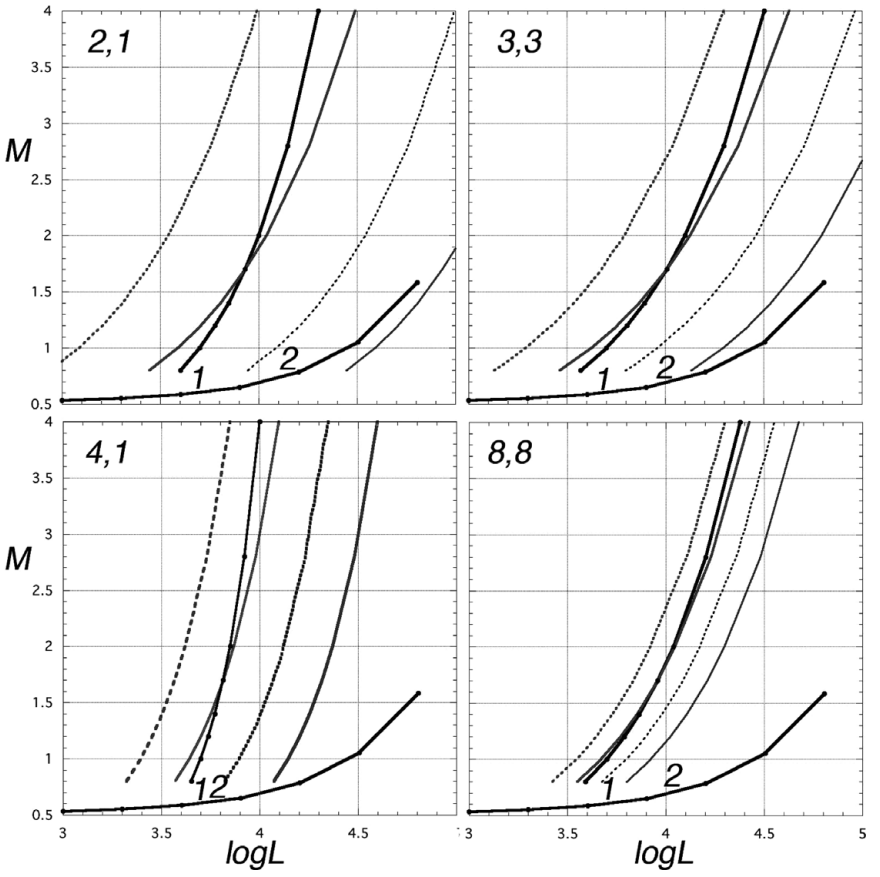

Figure 1. The location of the death line (bold) and contours of constant mass loss rate (from left to right, 3×10^{-8}, 3×10^{-7}, 3×10^{-6}, 3×10^{-5} $M_\odot$/yr) for four combinations of $b = d\log\dot{M}/d\log L$ along an evolutionary track and $c = d\log\dot{M}/d\log M$ at fixed L. Each figure is labeled with its (b, c). A simple core mass-luminosity relation (Paczyǹski 1970) is also shown (lowest curve) and the location on this curve of the final mass for initial masses 1 and 2. If we assume that the mass loss rate remains above 3×10^{-5} $M_\odot$/yr below 3×10^{-5} (green) line then where this line is more than 0.3 solar masses above the core mass line we satisfy the criterion discussed by Moe (these proceedings) for PN progenitors. For large slopes, the results are relatively insensitive to the precise values as the mass loss contours are already very closely spaced. The slope of the initial-final mass relation at a given $L_{\rm death}$ depends on the ratio of c/b.

atmospheric densities. The first condition is based on Cox & Guili's (1968) suggestion that the maximum work done on/by the piston should not exceed $L_{\rm star}$. The second condition scales the piston amplitude to the speed of sound, assuming it should not become supersonic. These two conditions give rise to different slopes $d\log\dot{M}/d\log L$ along an evolutionary track: Mean values ∼16 for the power condition vs. ∼8 for the sound speed condition. In future grids we intend to try a smooth transition from the power limit condition to the sound speed limit as the amplitude of the piston approaches the sound speed. We note that most other modelers have used either constant piston velocity amplitude or a grid of values; the sound speed condition is actually quite close to a constant value of about 8 km/s.

For large $d\log\dot{M}/d\log L$ most parameters do not have the leverage to change $L_{\rm death}$ by very much, because $d\log L_{\rm death}/d\log X = (d\log\dot{M}/\log X)/(d\log\dot{M}/d\log L)$. The

https://doi.org/10.1017/S1743921312010721 Published online by Cambridge University Press

Table 1. Different mass-loss descriptions.

Mass loss formula	$\frac{d \log \dot{M}}{d \log L}$ for const. M	$\frac{-d \log \dot{M}}{d \log M}$ for $M > 1.2$[a]
Reimers 1975	1.68	1.31
Schröder & Cuntz 2005	2.672	1.71
Blöcker 1995	4.38	1.31
Wachter *et al.* 2002	3.1	3.0
Vassiliadis & Wood 1993	13.6	10
WWB – power[b]	16	19
WWB – sound[b]	8	12

Notes:
[a]By the Iben (1984) formula we use to relate R to L, M, Z and l/H, $d \log R/d \log M = 0$ for $M < 1.175$ and 0.31 for $M > 1.175$. This influences $d \log \dot{M}/d \log M$ for any formula involving R, $T_{\rm eff}$, or pulsation period.
[b]WWB (= Willson & Wang, in prep) – power assumes that the piston power scales with the stellar luminosity. WWB – sound assumes that the piston amplitude is equal to the speed of sound at the piston. We expect the power condition to be most appropriate for models with small mean opacity or lower mass loss rate, and the amplitude condition to be appropriate for higher mean opacity, higher $\dot{M}$ models

parameters with the most leverage are mixing length (varying R at fixed L, M, Z), metallicity (also because it alters R as well as dust and molecular opacity), and mean opacity κ (because the photospheric density $\rho_{\rm phot} = (2/3)/\kappa H$ where H = scale height at the photosphere). In Figures 2 and 3 we show the density and the local mean mass loss rate vs. radius for three κ values at fixed metallicity. Varying the onset of non-LTE, or varying the condensation temperature for dust grains, within a reasonable range of values have remarkably small effect on the mass loss rates, although they do make a considerable difference in the atmospheric temperature and velocity structure.

For the purpose of PN studies, we need to know both the mass loss rate during the loss of the last few tenths of a solar mass of envelope and the amount of envelope mass left when the AGB wind terminates. The latter quantity, together with $M_{\rm core}$, determines the time delay between leaving the AGB and reaching the temperature of PNNi; the former, the amount of material still close enough for the central star to ionize it and/or for the fast wind to catch up to it. These are very hard quantities to obtain from current mass loss models, however. The analysis above gives upper and lower limits but no firm answers yet. Current models do not give a very accurate picture of very high mass loss rates; the Bowen code, for example, does not do well for mass loss rates much above 10^{-5} $M_\odot$/yr. It is also quite possible, as suggested by Vassiliadis & Wood (1993), that there is a maximum steady mass loss rate that is achieved – perhaps different for M and C stars – that is between 10^{-5} and 10^{-4} $M_\odot$/yr. After all, an optically thin outflow driven by radiation has $\dot{M} \lesssim L/cv_\infty$ which at 5000 $L_\odot$ with $v_\infty = 10$ km/s is $\dot{M} = 10^{-5}$ $M_\odot$/yr. If there is a maximum mass loss rate, then the mass available to form a PN will depend on this final mass loss rate and on the envelope mass left when the AGB mass loss stops. This, in turn, depends on how the star responds to loss of mass as the envelope mass becomes very low. In evolutionary models, the radius vs. envelope mass curve has 3 parts: R increasing with decreasing M; R decreasing slowly with decreasing M; R decreasing rapidly with decreasing M (Frankowski 2003, see Figure 4). For the example in the figure we have assumed $\dot{M} = 3 \times 10^{-8} (R/300)^{10} (M/M_\odot)^{10}$ at $\log(L/L_\odot) = 3.7$. The luminosity is kept constant over the episode of mass loss to get a sense of how R and M will influence

https://doi.org/10.1017/S1743921312010721 Published online by Cambridge University Press

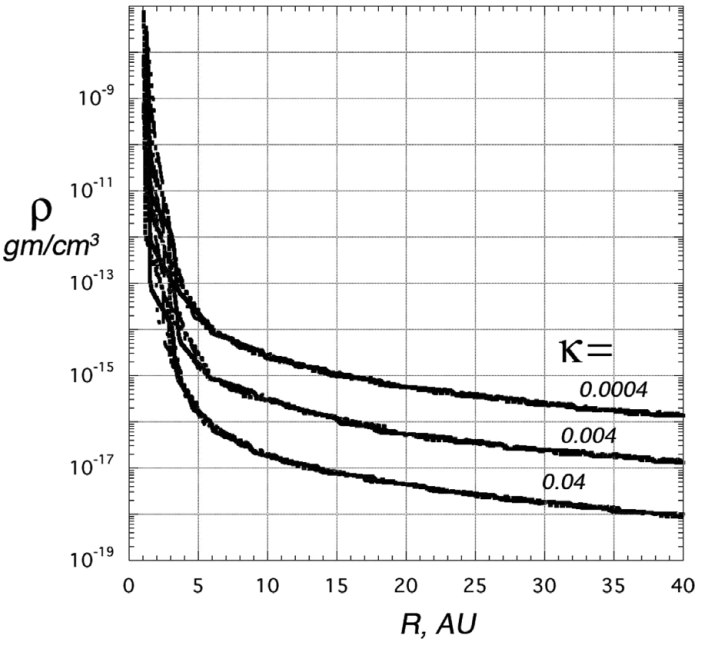

Figure 2. Density vs. radial position is plotted for 4 phases of three models that are identical except for the assume mean opacity. The photospheric density scales with $1/\kappa$ and so does the wind density for most cases we have examined. A mean opacity of 0.0004 cm^2/g is close to the expected photospheric Rosseland mean opacity for an M-star near the tip of the AGB, while 0.04 cm^2 is closer to the Planck mean opacity.

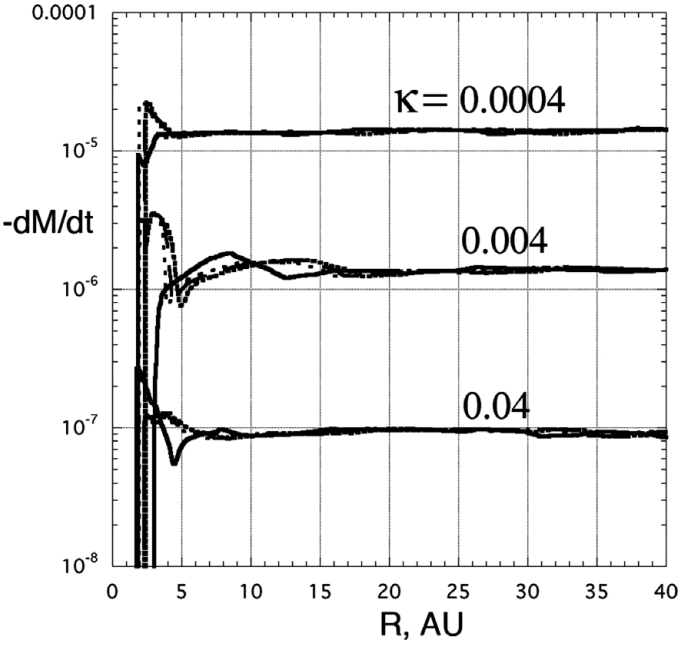

Figure 3. Mass loss rate $4\pi r^2 \rho v$ vs. radius for the same models as are shown in Figure 2. The main effect of varying κ on the mass loss rate comes from the change in the photospheric density see in Figure 2.

https://doi.org/10.1017/S1743921312010721 Published online by Cambridge University Press

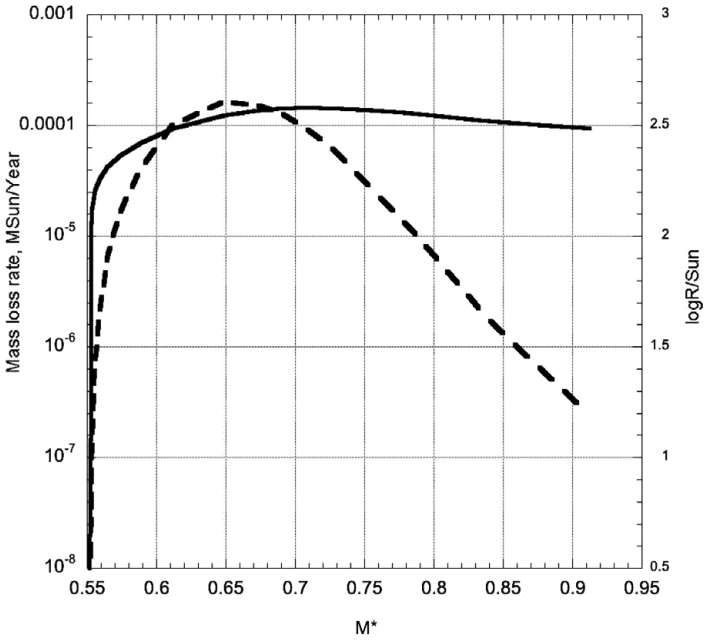

Figure 4. An example of how the radius and the resulting mass loss rate may vary with decreasing stellar mass for a star with a core mass of 0.55 solar masses, $\log(L/L_\odot) = 3.7$, and an assumed mass loss law $= 5 \times 10^{-8}(R/300)^{10}(M/M_\odot)^{-15}$ $M_\odot$/yr – chosen to produce a peak rate of a few $\times 10^{-5}$ $M_\odot$/yr. This illustrates how the decreasing radius ultimately offsets the decreasing mass and effectively ends the steady AGB mass loss while the envelope mass is still too large to allow rapid evolution to the blue of the central star.

the mass loss rate at the end. In this example, and probably also in reality, steady AGB mass loss will end when the envelope mass is $\gtrsim 0.02$ $M_\odot$, leaving the star unable to make a rapid transition to the blue. However, a transient response to rapid changes in R could lead to ejection of more mass at the end.

4. Conclusions

With a large grid of models we investigate the influence of various physical processes on the mass loss rates of AGB tip stars. We find that knowing the radius $R(L, M, Z)$ is critical to predicting $L_{\rm death}(M, Z)$, and that the dependence of R on Z has a large effect on the mass loss rate. We confirm that most mass loss formulae and most model results give reasonable death lines and thus about the same PNN masses, if this process leads to PNe. The minimum progenitor mass that can produce a PN of a given mass depends mostly on the exponent $d\log\dot{M}/d\log M$ and the slope $d\log\dot{M}/d\log L$ along an evolutionary track. The mass actually available to form a PN is harder to predict; we can most easily obtain an upper limit from current models.

Acknowledgements

The work we are doing is built on the legacy left by George Bowen. Useful discussions have been held with Massimo Marengo, Steve Kawaler, and Curt Struck. We acknowledge support from NSF grant 0708143. We would also like to thank the organizers for inviting us to beautiful Tenerife for this conference.

References

Blöcker, T. 1995, *A&A*, 297, 727
Bowen, G. H. 1988, *ApJ*, 329, 299
Cox, J. P. & Giuli, R. T. 1968, *Principles of Stellar Structure*, Gordon & Breach.
Fleischer, A. J., Gauger, A., & Sedlmayr, E. 1992, *A&A*, 266, 321
Frankowski, A. 2003, *A&A*, 406, 265
Gail, H.-P. & Sedlmayr, E. 1999, *A&A*, 347, 594
Hill, S. J. & Willson, L. A. 1979, *ApJ*, 229, 1029
Höfner, S. 2009, *Cosmic Dust - Near and Far*, 414, 3
Höfner, S., Gautschy-Loidl, R., Aringer, B., & Jørgensen, U. G. 2003, *A&A*, 399, 589
Höfner, S. & Dorfi, E. A. 1997, *A&A*, 319, 648
Höfner, S., Feuchtinger, M. U., & Dorfi, E. A. 1995, *A&A*, 297, 815
Iben, I., Jr. 1984, *ApJ*, 277, 333
Marigo, P. 2002, *A&A*, 387, 507
Mattsson, L., Wahlin, R., & Höfner, S. 2010, *A&A*, 509, A14
Mattsson, L. & Höfner, S. 2011, *A&A*, 533, A42
Olofsson, H., Carlstrom, U., Eriksson, K., Gustafsson, B., & Willson, L. A. 1990, *A&A*, 230, L13
Paczyński, B. 1970, *ACTAA*, 20, 47
Reimers, D. 1975, *Memoires of the Societe Royale des Sciences de Liege*, 8, 369
Schröder, K.-P. & Cuntz, M., 2005, *ApJ*, 630, L73
Vassiliadis, E. & Wood, P. R. 1993, *ApJ*, 413, 641
Wachter, A., Schröder, K.-P., Winters, J. M., Arndt, T. U., & Sedlmayr, E. 2002, *A&A*, 384, 452
Willson, L. A. 2007, *Why Galaxies Care About AGB Stars: Their Importance as Actors and Probes*, 378, 211
Willson, L. A. 2000, *ARAA*, 38, 573
Willson, L. A. & Hill, S. J. 1979, *ApJ*, 228, 854
Woitke, P. 2006, *A&A*, 460, L9
Wood, P. R. 1979, *ApJ*, 227, 220